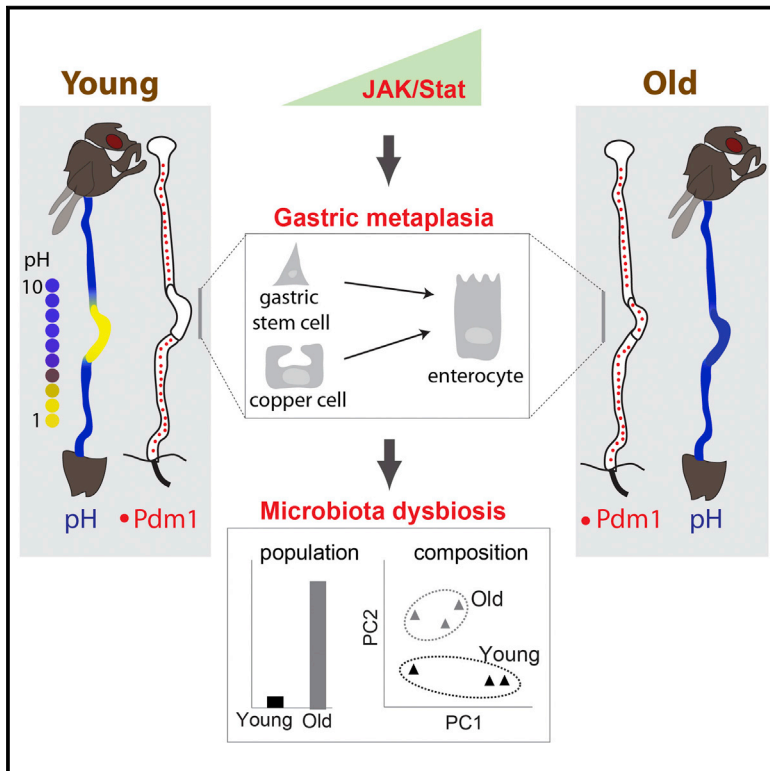


# Cell Host & Microbe

## Preventing Age-Related Decline of Gut Compartmentalization Limits Microbiota Dysbiosis and Extends Lifespan

### Graphical Abstract



### Authors

Hongjie Li, Yanyan Qi, Heinrich Jasper

### Correspondence

hjasper@buckinstitute.org

### In Brief

Age-related commensal dysbiosis in the intestine has been linked to shorter lifespan, but the underlying mechanisms remain unclear. Li et al. find that a JAK/Stat-mediated epithelial metaplasia disrupts gastrointestinal compartmentalization, leading to microbiota dysbiosis in old *Drosophila*. Accordingly, limiting JAK/Stat activity is sufficient to improve gut function and extend lifespan.

### Highlights

- GI compartmentalization controls intestinal microbiota
- GI compartmentalization declines with age due to gastric metaplasia
- Age-related activation of JAK/Sat signaling leads to gastric metaplasia
- Limiting JAK/Stat in the gastric region prevents dysbiosis and extends lifespan



# Preventing Age-Related Decline of Gut Compartmentalization Limits Microbiota Dysbiosis and Extends Lifespan

Hongjie Li,<sup>1,2</sup> Yanyan Qi,<sup>1</sup> and Heinrich Jasper<sup>1,2,\*</sup>

<sup>1</sup>Buck Institute for Research on Aging, 8001 Redwood Boulevard, Novato, CA 94945-1400, USA

<sup>2</sup>Department of Biology, University of Rochester, River Campus Box 270211, Rochester, NY 14627, USA

\*Correspondence: [hjasper@buckinstitute.org](mailto:hjasper@buckinstitute.org)

<http://dx.doi.org/10.1016/j.chom.2016.01.008>

## SUMMARY

Compartmentalization of the gastrointestinal (GI) tract of metazoans is critical for health. GI compartments contain specific microbiota, and microbiota dysbiosis is associated with intestinal dysfunction. Dysbiosis develops in aging intestines, yet how this relates to changes in GI compartmentalization remains unclear. The *Drosophila* GI tract is an accessible model to address this question. Here we show that the stomach-like copper cell region (CCR) in the middle midgut controls distribution and composition of the microbiota. We find that chronic activation of JAK/Stat signaling in the aging gut induces a metaplasia of the gastric epithelium, CCR decline, and subsequent commensal dysbiosis and epithelial dysplasia along the GI tract. Accordingly, inhibition of JAK/Stat signaling in the CCR specifically prevents age-related metaplasia, commensal dysbiosis and functional decline in old guts, and extends lifespan. Our results establish a mechanism by which age-related chronic inflammation causes the decline of intestinal compartmentalization and microbiota dysbiosis, limiting lifespan.

## INTRODUCTION

The intestinal microbiota influences long-term homeostasis of metazoans by maintaining epithelial integrity in the GI tract, supporting digestion, training the intestinal immune system, and preventing the growth of pathogenic bacteria (Clemente et al., 2012). The composition of the gut microbiota is influenced by the interaction with GI epithelia and by a range of genetic and environmental factors (David et al., 2014; Clemente et al., 2012). Alteration of microbiota composition (“dysbiosis”) has been associated with numerous pathologies and with aging (Clemente et al., 2012; Claesson et al., 2011, 2012). While preventing commensal dysbiosis in aging flies extends lifespan, its origin is unknown (Buchon et al., 2013; Clark et al., 2015; Guo et al., 2014).

The GI tract of most animals is lined by a series of highly specialized epithelia that perform localized functions but have

common characteristics to manage the commensal population, allow immune responses to infections, and maintain intestinal barrier function (Barker et al., 2010; Buchon et al., 2013; Li et al., 2013; Marianes and Spradling, 2013; Strand and Micchelli, 2011). How compartmentalization influences the microbiota, and whether age-related changes in compartment identities contribute to age-related dysbiosis, remains unknown.

The adult *Drosophila* intestine constitutes a genetically accessible model system to address these questions. Studies exploring age-related changes in epithelial homeostasis, regenerative capacity, stem cell (SC) function, host-commensal interactions, and innate immune signaling have provided rich insight into mechanisms governing intestinal homeostasis (Ayyaz and Jasper, 2013; Biteau et al., 2011a; Lemaitre and Miguel-Aliaga, 2013). Based on morphological and functional characteristics, the midgut of flies can be subdivided roughly into the anterior midgut (AM), the middle midgut (MM), which contains an acidic gastric or copper cell region (CCR [Dubreuil, 2004]), and the posterior midgut (PM; Figure 1A). Finer subdivisions into 10–14 regions have been described based on more detailed morphological and molecular landmarks along the GI tract (Buchon et al., 2013; Marianes and Spradling, 2013). Intestinal SCs (ISCs) can be found in each of these compartments (Biteau et al., 2011a; Strand and Micchelli, 2011). ISCs in the PM express escargot (esg) and Delta (Dl) and divide asymmetrically to give rise to precursor cells (the Dl<sup>−</sup>/esg<sup>+</sup> Enteroblasts, EBs), which will further differentiate into either Pdm1-expressing Enterocytes (ECs) or prospero (pros)-expressing Enteroendocrine cells (EEs) (Ayyaz and Jasper, 2013; Biteau et al., 2011a; Lemaitre and Miguel-Aliaga, 2013). In the CCR, esg<sup>+</sup> gastric stem cells (GSSCs) respond to stress by inducing regeneration of three different cell types: Dve<sup>+</sup>/Labial<sup>+</sup>/Cut<sup>+</sup> Copper cells (CCs, which secrete hydrochloric acid), Dve<sup>+</sup>/weak Labial<sup>+</sup>/Cut<sup>−</sup> interstitial cells, and Pros<sup>+</sup> EEs (Strand and Micchelli, 2011) (Figure S2A). A gradient of the morphogen Decapentaplegic (Dpp), a *Drosophila* Bmp2/4 ortholog, segregates GSSCs from posterior midgut ISCs (Li et al., 2013).

The aging *Drosophila* intestine develops an inflammatory condition that is characterized by immune dysfunction, commensal dysbiosis, and intestinal stem cell (ISC) over-proliferation (Biteau et al., 2011b; Buchon et al., 2009; Clark et al., 2015; Guo et al., 2014). This results in metabolic decline and is associated with loss of the intestinal barrier function, promoting mortality in aging animals (Ayyaz and Jasper, 2013; Biteau et al., 2010, 2011a; Guo et al., 2014; Lemaitre and Miguel-Aliaga, 2013; Rera et al., 2012).

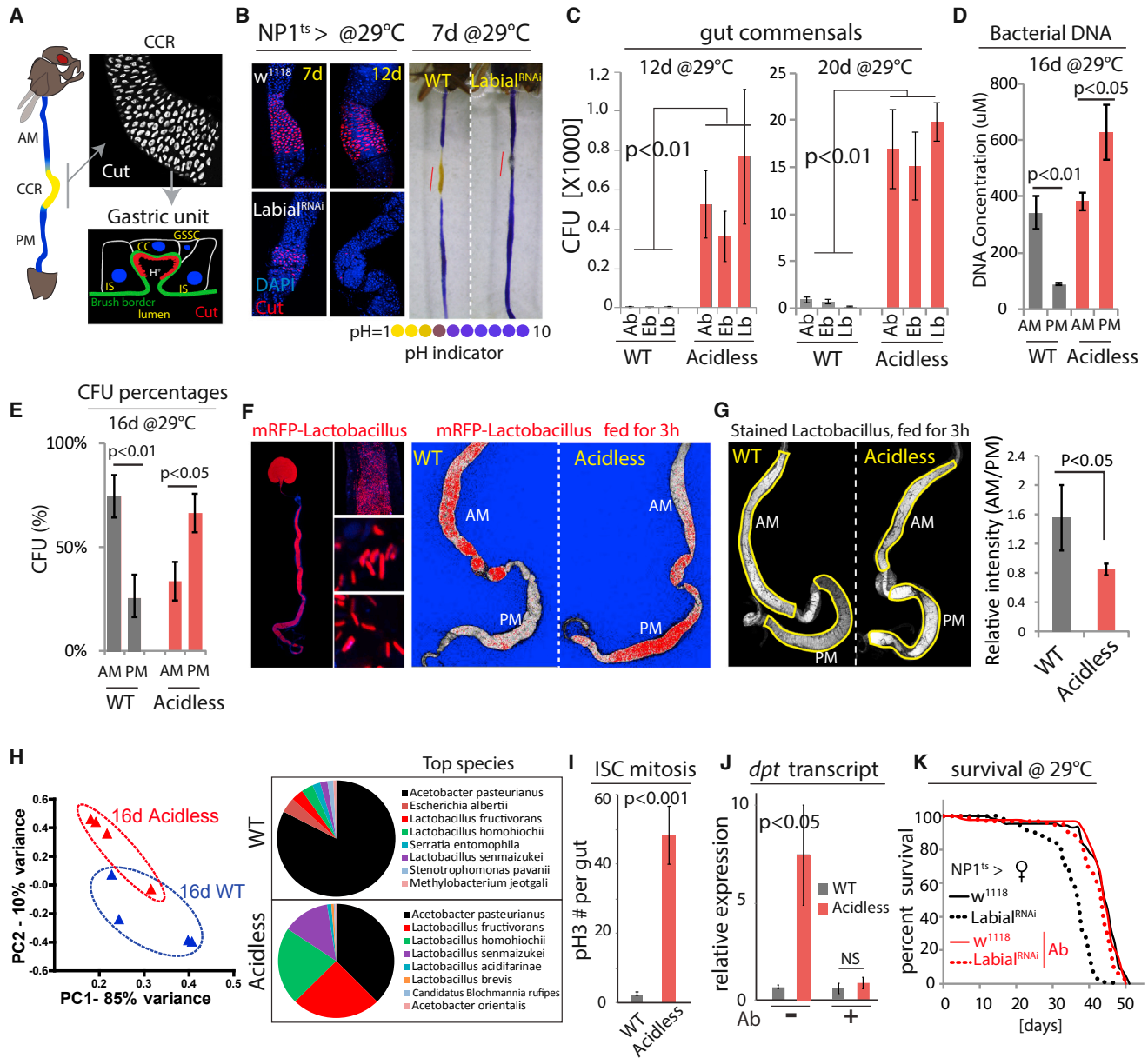


**Figure 1. Intestinal Compartmentalization Impacts Gut Microbiota**

(A) Left: the *Drosophila* GI tract consists of anterior midgut (AM), middle midgut (MM) with copper cell region (CCR), and posterior midgut (PM). Right: anti-Cut (white) labels acid-producing copper cells (CCs). A gastric unit. IS, interstitial cell; GSSC, gastric stem cell.

(B) Expression of *Labial<sup>RNAi</sup>* results in loss of CCs. Acidic regions (yellow) indicated by pH indicator Bromophenol blue. Representative images of three independent experiments.  $n = 7$  for each genotype and time point.

(C) Commensal numbers in 12-day- and 20-day-old WT ( $NP1^{ts}>w^{1118}$ ) and acidless flies ( $NP1^{ts}>Labial^{RNAi}$ ). Colony-forming units (CFUs) of three common commensal phylotypes (Acetobacter, Ab; Enterobacter, Eb; Lactobacillus, Lb) are quantified using selective plates. Averages and SEM (t test),  $n = 6, 6, 6, 10, 10$  (both 12 days and 20 days). Representative from three independent experiments.

(D) Bacterial DNA concentration of the AM and PM from 16-day-old WT and acidless flies. Averages and SEM (t test),  $n = 3 \times 10$  guts each.

(E) Commensal distribution in 16-day-old WT and acidless guts. Percent averages of colony-forming units (CFUs) in AMs and PMs are shown.  $n = 12, 11$ . Averages and SEM (t test).

(F) Distribution of RFP-tagged *Lactobacillus plantarum* in 16-day-old WT and acidless flies. Left: representative images of RFP-tagged *Lactobacillus* in the gut. Right: representative saturation images of WT and acidless guts with RFP-tagged *Lactobacillus*. Saturated signal red, un-saturated signal white, and background blue. False color images generated from confocal images in ZEN. Representative of three independent experiments.

(G) Distribution of stained *Lactobacillus* (by SYTO 9) in 16-day-old WT and acidless flies. Relative fluorescent intensity is quantified.  $n = 6, 9$ . Averages and SEM (t test).

(H) Commensal composition of 16-day-old WT and acidless guts. Principal component analysis (PCA) based on percentages of classified bacterial species determined by 16S rRNA sequencing. Pie charts show top bacterial species. For PCA, each dot represents ten guts; for pie charts, each represents the average of four samples ( $4 \times 10$  guts).

(legend continued on next page)

Interventions that limit dysbiosis and ISC over-proliferation extend lifespan (Biteau et al., 2010; Clark et al., 2015; Guo et al., 2014), yet the underlying cause for the age-related loss of intestinal homeostasis remains unclear. Previous studies have found that intestinal compartmentalization declines with age (Buchon et al., 2013) and that loss of Caudal, a transcription factor specifically expressed in the posterior midgut, impacts immune homeostasis and commensal composition (Ryu et al., 2008). Whether and how GI compartmentalization impacts the microbiota, whether changes in GI compartmentalization are associated with aging, and whether such changes influences longevity in flies has not been tested.

## RESULTS

### Gut Compartmentalization and Microbiota

To characterize the importance of GI compartmentalization for the maintenance and composition of the gut microbiota, we generated flies in which the stomach-like CCR was specifically ablated by knocking down Labial using NP1::Gal4, tub::Gal80<sup>ts</sup>, a temperature-sensitive driver that is specific for differentiated cells in the gut (McGuire et al., 2004a; this combination is referred to as NP1<sup>ts</sup>; Figures 1B, S1A, and S1B). Since Labial is required for CC maintenance (Buchon et al., 2013; Li et al., 2013), this results in rapid decline of CCs, and a corresponding loss of acidity in the MM. In these “acidless” flies, the expression of the CC-specific vacuolar-type H<sup>+</sup> ATPase, *Vha100-4*, was significantly reduced compared to controls, confirming the loss of CCs (Figures S1D and S1E).

In acidless flies, the number of colony-forming units (CFUs) of the three main commensal phylotypes (Lactobacilli, Acetobacilli, and Enterobacteria) increased significantly (Figures 1C, S1C, S1F, and S1G). Since commensals in flies are only weakly associated with the gut and need continuous reconstitution by ingestion (Blum et al., 2013; Broderick et al., 2014), we hypothesized that the CCR manages survival of ingested bacteria and colonization of the PM. Supporting this hypothesis, the bacterial load (the number of CFUs, or the concentration of bacterial DNA) is higher in the AM than the PM of wild-type flies, but this relationship is reversed in acidless flies (Figures 1D, 1E, and S1H; note that there is also an increase in commensals in the AM in acidless animals, potentially due to re-ingestion of excreted bacteria, or due to immune dysfunction triggered by elevated Foxo activity in ECs of the AM, see below). Furthermore, the distribution of RFP-tagged commensal *Lactobacillus plantarum* isolated from wild-type flies and re-introduced into wild-type or acidless flies is strongly impacted by the CCR: tagged bacteria are enriched in the AM of wild-type flies but are predominantly localized in the PM of acidless flies (Figures 1F and S1I). The same was observed using *Lactobacilli* stained by a fluorescent dye (Figure 1G).

16S rRNA gene sequencing revealed a significant difference in microbiota composition between wild-type and acidless guts,

reflecting a strong enrichment of *Lactobacilli* at the expense of *Acetobacteria* (Figure 1H). Acidless flies further exhibit increased expression of the Foxo target gene *thor* (Figures S1J and S1K; note that the most obvious increase was seen in the AM and the posterior PM) and of the anti-microbial peptide *Diptericin* (*Dpt*), as well as higher rates of ISC proliferation compared to wild-type (as determined by quantifying mitotic figures, phospho-Histone H3-expressing cells, Figures 1I, 1J, and S1L). These phenotypes are reminiscent of the loss of intestinal homeostasis in aging animals, which is characterized by elevated Foxo activity in ECs, resulting in hyperactivation of the Relish/NFκB signaling pathway (which induces *Dpt*), commensal dysbiosis, and ISC hyperactivation (Guo et al., 2014). Accordingly, acidless flies exhibit shorter lifespan than controls (Figure 1K). Antibiotic treatment is sufficient to reduce *Dpt* expression and restores wild-type lifespan in acidless animals (Figures 1J and 1K), confirming that commensal dysbiosis triggers these phenotypes.

### Age-Related Gastric Decline and Metaplasia

Since these results uncovered a critical role for the CCR in managing the microbiota, and since acidless flies exhibited phenotypes reminiscent of old flies, we assessed CCR function in aging wild-type flies. We find that the size of the CCR and the structure of gastric units decline with age in both conventionally and axenically reared animals (Figures 2A and 2B). This is associated with reduced expression of *Vha100-4* (Figures 2C and S2B), and with accumulation of Pdm1+ cells in the CCR (Figures 2D, S2C, and S2D).

*Vha100-4* is a member of a family of vacuolar-type H<sup>+</sup> ATPases encoded in the fly genome. *Vha16-1* has been reported to be expressed in the CCR based on a Gal4 trap line and to be required to maintain gut acidity (Lin et al., 2015). However, our RT-PCR and RNA-seq data indicate that *Vha100-4*, which is highly enriched in the CCR (Figure 2C), is the only *Vha* gene with decreased expression in guts of acidless flies (Figure S1D). Another study (Buchon et al., 2013) has found high specific *Vha100-4* expression in the CCR, while *Vha16-1* cannot be detected. Systematic analysis of *Vha* genes and their relative functions in the fly gut is of interest for future studies.

Pdm1 (also called nubbin), a POU-domain homeobox transcription factor, is a widely used marker for ECs in the PM (Lee et al., 2009) (Figure S2D), and is required for their differentiation (Korzelius et al., 2014), but is not expressed in cells of the MM in young flies (Figures 2D and S2D; no change in Pdm1 expression is seen in the aging PM, Figure S2E). The appearance of ectopic Pdm1+ cells suggested that the age-related decline of the CCR is the result of a metaplasia (a condition in which epithelial subtypes acquire ectopic properties) in which CCs in the MM are replaced by Pdm1+ EC-like cells characteristic of the PM epithelium.

Since this gastric decline occurs in both axenic and conventional conditions, it is likely a cause, not a consequence, of the age-related loss of intestinal homeostasis. Supporting this

(I) Quantification of pH3+ cells in guts of 16-day-old flies at 29°C. Averages and SEM (t test); n = 12, 11. Data are representative of three independent experiments.

(J) qRT-PCR showing *dpt* expression of 16-day-old flies on normal or antibiotic (Ab) food. Averages and SEM (t test) of n = 3 biological replicates.

(K) Lifespan of acidless flies compared to WT controls on normal or antibiotic (Ab) food. Without antibiotics: WT n = 88, acidless n = 93, Log-rank p value < 0.0001, 17.8% change of median lifespan; Antibiotics: WT n = 110, acidless n = 100, Log-rank p value = 0.02, no change of median lifespan.

See also Figure S1.

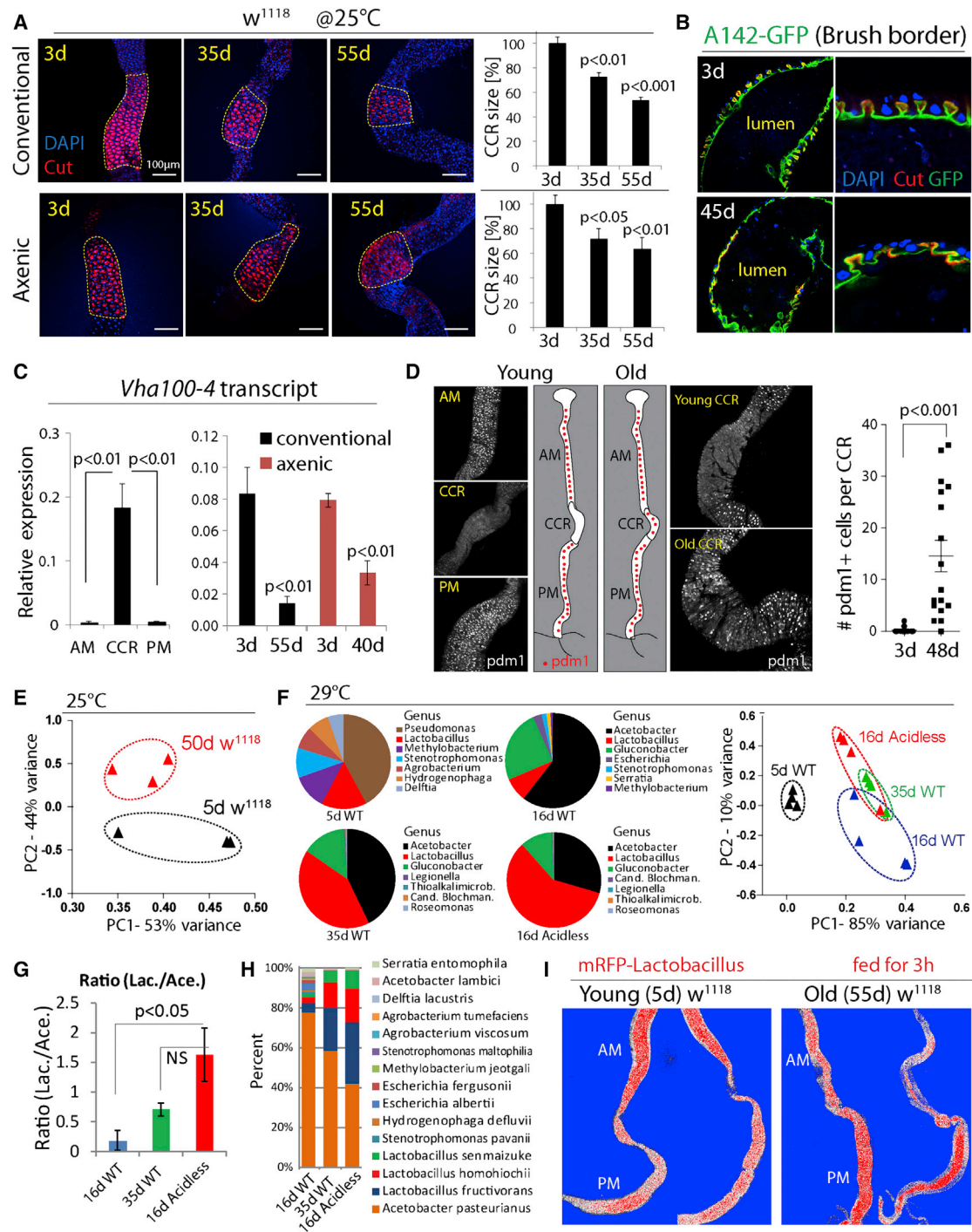


**Figure 2. Age-Related Gastric Decline and Metaplasia**

(A) CCRs (outlined) of  $w^{1118}$  flies decline with age. CCR area is quantified on the right. Averages and SEM (t test) from one experiment representative of more than three independent repeats. Conventional:  $n = 5, 7, 7$ ; Axenic:  $n = 7, 11, 11$ .

(B) Age-related decline of gastric units of  $w^{1118}$  flies. Anti-Cut (red) and brush border (green, A142-GFP). Representative images of six flies at each age in two independent experiments.

(C) qRT-PCR measuring expression of *Vha100-4* (normalized to *actin5C*) in different regions of young  $w^{1118}$  flies (left) and in whole guts of  $w^{1118}$  flies (right). Averages and SEM (t test),  $n = 3$  biological replicates.

(D) Pdm1 expression along the GI tract. Representative images, experiment has been repeated at least three times in three wild-type genetic backgrounds ( $y^1, w^1/w^{1118}$ , *Dve::Gal4/+*,  $y^1, w^1/w^{1118}$ ;  $w^{1118}$ , *S*, 106::GS/+). Pdm1+ cells per CCR are quantified. Averages and SEM (t test),  $n = 20, 17$ .

(E) Principal component analysis (PCA) based on percentages of classified bacterial species from 5-day- and 50-day-old  $w^{1118}$  flies at 25°C. Each dot represents ten guts.

(legend continued on next page)

notion, the microbiota composition of young acidless animals resembles that of old wild-type flies more than that of wild-type flies of the same age (Figures 2E–1H, S2F, and S2G; the composition in old wild-type flies differs significantly from that of young wild-type flies reared at the same temperature). Furthermore, the anterior-posterior distribution of RFP-tagged *Lactobacillus* in old flies shows a pattern similar to that of acidless flies: tagged bacteria are enriched in the PM (Figures 1F and 2I).

### JAK/Stat Activation Causes CCR Metaplasia

Age-related metaplasia thus significantly perturbs commensal distribution, composition, and size and contributes to age-related intestinal dysfunction. To characterize the molecular mechanism causing this metaplasia, we explored signaling pathways whose activity changes with age in the gut of both axenically and conventionally reared animals (Guo et al., 2014). These pathways include JAK/Stat signaling, as illustrated by the fact that the expression of the JAK/Stat activity reporter 2xStat::GFP (Bach et al., 2007) increases throughout the gut (including the CCR) in flies aged under both conventional and axenic conditions (Figure 3A). This activation is likely a result of local and/or systemic induction of one of the three Unpaired ligands (Upd, Upd2, and Upd3) that activate JAK/Stat signaling in flies. Indeed, expression of *unpaired 3* (*upd3*) strongly increases with age in the gut, while *upd2* and *upd3* are significantly induced in the abdominal fatbody with age (Figures 3B and S3A).

Activation of JAK/Stat signaling in CCs of young guts by locally expressing Upd2 or Upd3 (using *Dve::Gal4*, which drives expression in differentiated cells of the MM, combined with *tub::Gal80<sup>ts</sup>*; Figure S3B), by cell-autonomously activating JAK (using *Dve<sup>ts</sup>* to express the constitutively active JAK/hopscotch mutant *Hop<sup>TumL</sup>* [Classen et al., 2009]), or by systemically elevating Upd2 expression (using the fatbody driver *ppl::Gal4<sup>ts</sup>*), resulted in strong metaplasia, widely replacing Cut+ cells by Pdm1+ cells in the MM (Figure 3C; *ppl<sup>ts</sup>*-mediated expression of Upd3 did not impact the gut, data not shown). Upd2 expression from fatbody is sufficient to activate JAK/Stat in the gut, as determined by the induction of the JAK/Stat target gene *Socs36E* (Figure S3D). Metaplasia was also observed when JAK/Stat was activated acutely in the intestine of young flies by exposure to Paraquat, which damages ECs and triggers regenerative responses by broadly activating JNK and JAK/Stat signaling in the gut (including in the visceral muscle, EBs, and ISCs; Figures 3C and S3C) (Biteau et al., 2008; Jiang et al., 2009; Osman et al., 2012; Zhou et al., 2013).

These data suggested that in old flies, both systemically and locally derived Upd ligands may contribute to constitutively activating JAK/Stat signaling in the gut, resulting in metaplasia of the CCR. Supporting this notion, knockdown of Stat, Hop, or the receptor Dome in MM cells limits age-related or Paraquat-induced

metaplasia (Figures 3D, S3C, S3G, and S3H), reduces the expression of JAK/Stat targets (*Socs36E*), and prevents the loss of *Vha100-4* expression in old guts (Figure 3E). A similar delay in the age-related decline of the CCR was observed in flies carrying the loss of function allele *hop<sup>3</sup>*, while flies carrying the gain-of-function allele *hop<sup>TumL</sup>* (a dominant gain-of-function mutation of the endogenous *hop* gene [Hanratty and Dearolf, 1993]) exhibited accelerated CCR decline (Figure S3I).

The specific contribution of locally and systemically derived Upds to gastric decline is likely to be complex and redundant: knockdown of Upd2 using *S<sub>1</sub>106-GeneSwitch* (a driver that allows strong RU486-mediated transgene induction in fatbody, but also some induction in the gut [Alic et al., 2014; Hwangbo et al., 2004]) extended lifespan of the animal overall but was not sufficient to prevent age-related metaplasia (Figures S3E and S3F). Other Upd ligands, or other sources of Upd2, are thus likely responsible for age-related gastric metaplasia, while the lifespan extension observed upon Upd2 knockdown in fatbody is independent of gastric decline and may be a consequence of Upd2-mediated systemic metabolic effects (Rajan and Perrimon, 2012). We observed no lifespan extension when Upd3 was knocked down using *S<sub>1</sub>106* (Figure S3E).

### Mechanism of JAK/Stat-Induced Metaplasia

The accumulation of Pdm1+ cells in the CCR may be the result of mis-differentiation of newly formed, GSSC-derived cells, or of trans-differentiation of established CCs into Pdm1+ cells. When *Hop<sup>TumL</sup>* was expressed in GSSCs and their daughter cells using *esg::Gal4* combined with *tub::Gal80<sup>ts</sup>* (*esg<sup>ts</sup>*) or in GSSC clones using the *esg<sup>ts</sup>F/O* lineage-tracing system (Jiang et al., 2009), newly formed cells became Pdm1+ (in both the PM and the CCR), while surrounding MM cells retained Cut staining, suggesting that *Hop<sup>TumL</sup>* can act cell autonomously in newly formed gastric cells to generate Pdm1+ polyploid cells (Figures 4C and S4A). Pdm1+ cells were also formed when *Hop<sup>TumL</sup>* was expressed selectively in GSSCs and not their daughter cells, using *esg<sup>ts</sup>* combined with *Su(H)::Gal80* (which inhibits Gal4 activity specifically in EBs and GBs [Wang et al., 2014]; Figure 4C). Elevated JAK/Stat activity within GSSCs is thus sufficient to convert these cells into PM-like ISCs that produce Pdm1+ EC-like cells rather than Cut+ CCs.

However, we also observed direct trans-differentiation of established CCs into Pdm1+ cells. Since *Dve::Gal4* is only expressed in differentiated, polyploid cells of the MM, it serves as an indicator of MM cell identity. Spontaneous Pdm1+ cells in the CCR of aging wild-type flies generally express low levels of *Dve*-driven GFP (Figure S4B), and co-expression of *Hop<sup>TumL</sup>* and GFP under the control of *Dve<sup>ts</sup>* results in progressive loss of the GFP signal and a corresponding increase in Pdm1 immunoreactivity (Figure S4C). The formation of Pdm1+ cells is thus accompanied by suppression of *Dve*.

(F) Pie charts show top bacterial genera of 5-day-old WT (*NP1<sup>ts</sup>>w<sup>1118</sup>*), 16-day-old WT, 16-day-old WT, and 16-day-old acidless (*NP1<sup>ts</sup>>Labial<sup>RNAi</sup>*) flies. Flies are cultured at 29°C to induce driver expression. PCA is based on percentages of classified bacterial species. For PCA, each dot represents 10 guts; for pie charts, each represents the average of four samples (40 guts).

(G and H) Ratios of total *Lactobacillus* and *Acetobacter* (G), and distribution of top 15 bacterial species (H), in flies of three conditions shown in (F). Averages and SEM (t test) for (G). Averages of four samples for (H).

(I) Change of *Lactobacillus* distribution in old guts (compare Figure 1F). See also Figure S2.

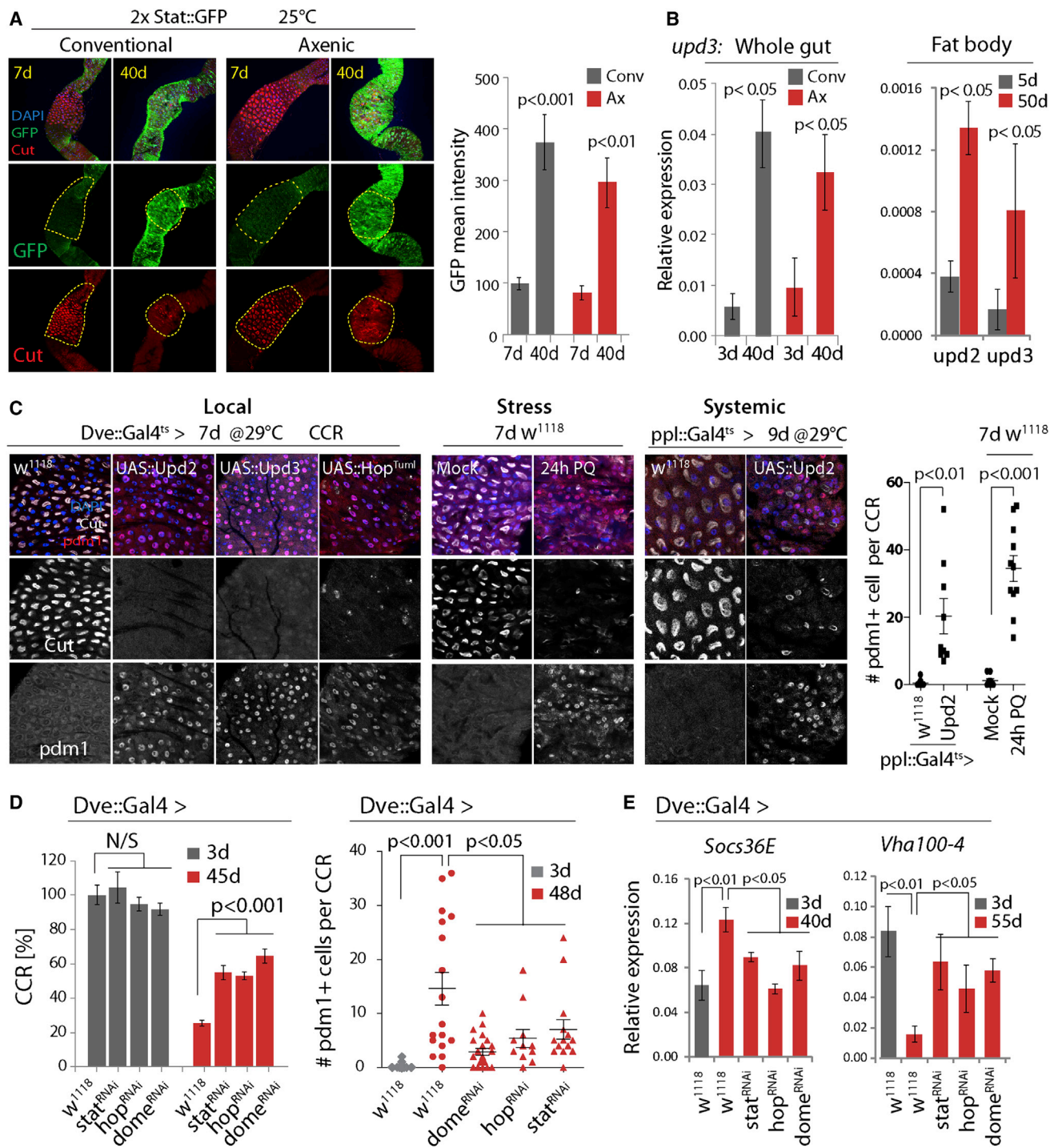


**Figure 3. Age-Related Activation of JAK/Stat Causes CC Loss and Metaplasia**

(A) Expression of 2xStat::GFP (green) in young and old CCRs. GFP intensity quantified on the right (normalized to 100 for young conv. condition). Averages and SEM (t test). Conv.: n = 8, 8. Axenic: n = 5, 9. Representative of three independent experiments.

(B) qRT-PCR measuring *upd3* expression (normalized to *actin5C*) in guts, and *upd2* and *upd3* in fat bodies, of *w<sup>1118</sup>* flies. Averages and SEM (t test). n = 3 biological replicates.

(C) Immunostaining detecting Cut+ CCRs and Pdm1+ cells in the CCR. Local: wild-type flies or flies overexpressing Upd2, Upd3, or Hop<sup>TumI</sup>. Stress: treatment with 80 mM Paraquat (PQ). Systemic: overexpression of Upd2 using the fat body driver *ppl::Gal4<sup>ts</sup>*. Quantifications of Pdm1+ cells per CCR from stress and systemic conditions are shown. Averages and SEM (t test), n = 12, 10, 10, 12. Data are representative of three independent experiments for Local, and two independent experiments for Stress and Systemic conditions.

(legend continued on next page)

The accumulation of Pdm1+ cells upon expression of Hop<sup>TumL</sup> is not accompanied by increased apoptosis (determined using Apoliner [Bardet et al., 2008], Figures 4A and S4D), nor does co-expression of the Caspase inhibitor P35 prevent the loss of CCs (Figure 4B, Hop<sup>TumL</sup> was expressed using NP1<sup>ts</sup> in this experiment). Consistently, while apoptosis increases in the PM of aging flies, we did not observe age-related increase of apoptosis in the CCR (determined by TUNEL staining, Figure S4E). Loss of Cut+ cells in response to JAK/Stat activation in CCs thus appears not to be driven by cell replacement, but rather by direct conversion of Cut+ cells into Pdm1+ cells. To test this hypothesis, we performed lineage tracing using G-Trace (Evans et al., 2009) and EdU incorporation experiments. In G-Trace, an inducible Gal4 (in our case Dve<sup>ts</sup>) activates expression of RFP in combination with UAS::Flp. Flp will then cause excision of a STOP-FRT cassette, allowing heritable expression of a ubiquitin-promoter-driven GFP. We shifted flies to 29°C to activate Dve::Gal4 for 3 days and then exposed them to Paraquat for 24 hr to induce JAK/Stat activity (Figure S5A). If Pdm1+ cells would be formed under these conditions directly from GSSCs (without going through a Dve+ state that is characteristic of MM cells), no Pdm1+ cell in the CCR should express GFP or RFP. However, only 10% of all Pdm1+ cells lacked GFP and RFP expression. Under stress conditions, the formation of Pdm1+ cells in the MM thus mostly involves transitioning through a Dve+ MM-like differentiated state (Figure 4D).

We further tested whether differentiated cells in the CCR can directly convert into Pdm1+ cells using EdU incorporation. A large majority of newly formed Pdm1+ cells did not incorporate EdU even when supplied for the full period of Hop<sup>TumL</sup> induction, indicating that no new DNA synthesis associated with polyploidization has occurred. Cut+ CCs can thus trans-differentiate into Pdm1+ cells rather than being replaced by new cells formed from GSSCs (Figure 4E).

Both mis-differentiation of GSSC-derived newly formed cells and trans-differentiation of established CCs can thus contribute to JAK/Stat-induced CCR metaplasia, suggesting that JAK/Stat signaling impairs molecular mechanisms that ensure formation and maintenance of CC identity. Dpp signaling is required for differentiation of CCs (Guo et al., 2013; Li et al., 2013), and the activity of Dpp signaling (pMad staining) is inhibited by JAK/Stat signaling in CCs (Figure S5B). This inhibition was rescued by knocking down the inhibitory SMAD Daughters against Dpp (Dad), suggesting a role for Dad in inhibiting Dpp signaling downstream of JAK/Stat activation in these cells (Figure S5B). Supporting this notion, activation of JAK/Stat signaling led to high expression of Dad::GFP in the CCR (Figure S5H). Inhibition of Dpp signaling, while preventing the formation of new Cut+ cells (Guo et al., 2013; Li et al., 2013) did not, however, cause the formation of Pdm1+ cells in the CCR: MARCM clones generated by ISCs homozygous for the *mad*<sup>72</sup> loss-of-function allele, while containing Pdm1+ cells in the PM did not contain such cells in the CCR (Figure S5C). Thus, inhibition of Dpp signaling, which

was also seen in old CCRs (Figure S5G), contributes to the loss of CCs, but not to the formation of Pdm1+ cells. Furthermore, knocking down Dad was not sufficient to rescue the UAS::Hop<sup>TumL</sup>-induced loss of CCs (Figure S5B), indicating that other mechanisms must act in parallel to perturb CC maintenance in JAK/Stat gain-of-function conditions.

The transcription factors Dve and Labial are both expressed specifically in polyploid cells, including CCs, of the MM. Consistent with the suppression of Dve expression in Pdm1+ CCs (Figure S4C), Dve transcripts in the CCR are reduced or increased when Hop<sup>TumL</sup> or Stat<sup>RNAi</sup> are expressed, respectively (Figure 4F). Similarly, Labial expression is repressed in GSSC lineages expressing Hop<sup>TumL</sup> (*esg*<sup>ts</sup>F/O; Figures 4F and S5D). Knockdown of either Dve or Labial using Dve<sup>ts</sup> results in the formation of Pdm1+ cells and loss of CCs (Figures 4G and 4H), and Labial-deficient Pdm1+ cells exhibit low Dve::Gal4 activity, while knockdown of Dve reduces Labial expression (Figures 4H and S5E). Knockdown of Dve did not, however, affect Dpp signaling as determined by pMad staining (Figure S5F).

We propose that CC identity is established and maintained by the co-dependent expression of Dve and Labial and that excessive JAK/Stat activation promotes trans-differentiation of CCs by independently perturbing the Labial-Dve network and Dpp signaling (Figure 4I).

### Inhibiting JAK/Stat Signaling Promotes Gut Homeostasis and Extends Lifespan

To test the importance of JAK/Stat-mediated metaplasia in the development of age-related intestinal dysfunction, we reduced JAK/Stat activity in the CCR and assessed age-related phenotypes in the gut. More than 90% of wild-type flies lose pH homeostasis with age (Figures 5A, 5B, and S6A). However, the observed phenotypes are not uniform: 44% of 45-day-old flies had a highly basic gut with no acidic region, while 46% exhibited weak staining throughout the gut (Figures 5A, 5B, and S6A). While the loss of the acidic region was expected based on the observed decline of the CCR, the loss of staining in other flies was surprising, and further analysis suggested that it is caused by the age-related expansion of acid-producing commensals, like *Lactobacillus*: when old flies were treated with antibiotics, the proportion of flies with reduced staining declined, while flies with a more basic gut lumen increased (Figure 5B and S6A). Furthermore, feeding young flies *Lactobacilli* cultured from fly guts (these cultures themselves have a pH of around 4) resulted in an intestinal pH pattern that was similar to old flies with increased intestinal acidity (Figure S6B; *Lactobacillus* readily colonized these guts, Figure S6C). Ingestion of a blue food dye confirmed that these flies took in similar amounts of food as sucrose-fed animals (Figure S6B). The loss of staining in old guts is thus due to *Lactobacillus*-induced luminal changes or a bacteria-induced barrier dysfunction.

Knocking down JAK/Stat signaling components using Dve::Gal4 restored pH homeostasis, limited commensal dysbiosis,

(D) Knockdown of JAK/Stat signaling components limits age-induced gastric decline. Left: n = 12, 11, 11, 12, 20, 20, 16, 22. Right: n = 20, 17, 22, 12, 15. Averages and SEM (t test). Representative from three independent experiments.

(E) qRT-PCR detecting *Socs36E* and *Vha100-4* in guts of wild-type (*w*<sup>1118</sup>) or Stat<sup>RNAi</sup>, Hop<sup>RNAi</sup>, or Dome<sup>RNAi</sup>-expressing flies. Averages and SEM (t test). n = 3 biological replicates.

See also Figure S3.



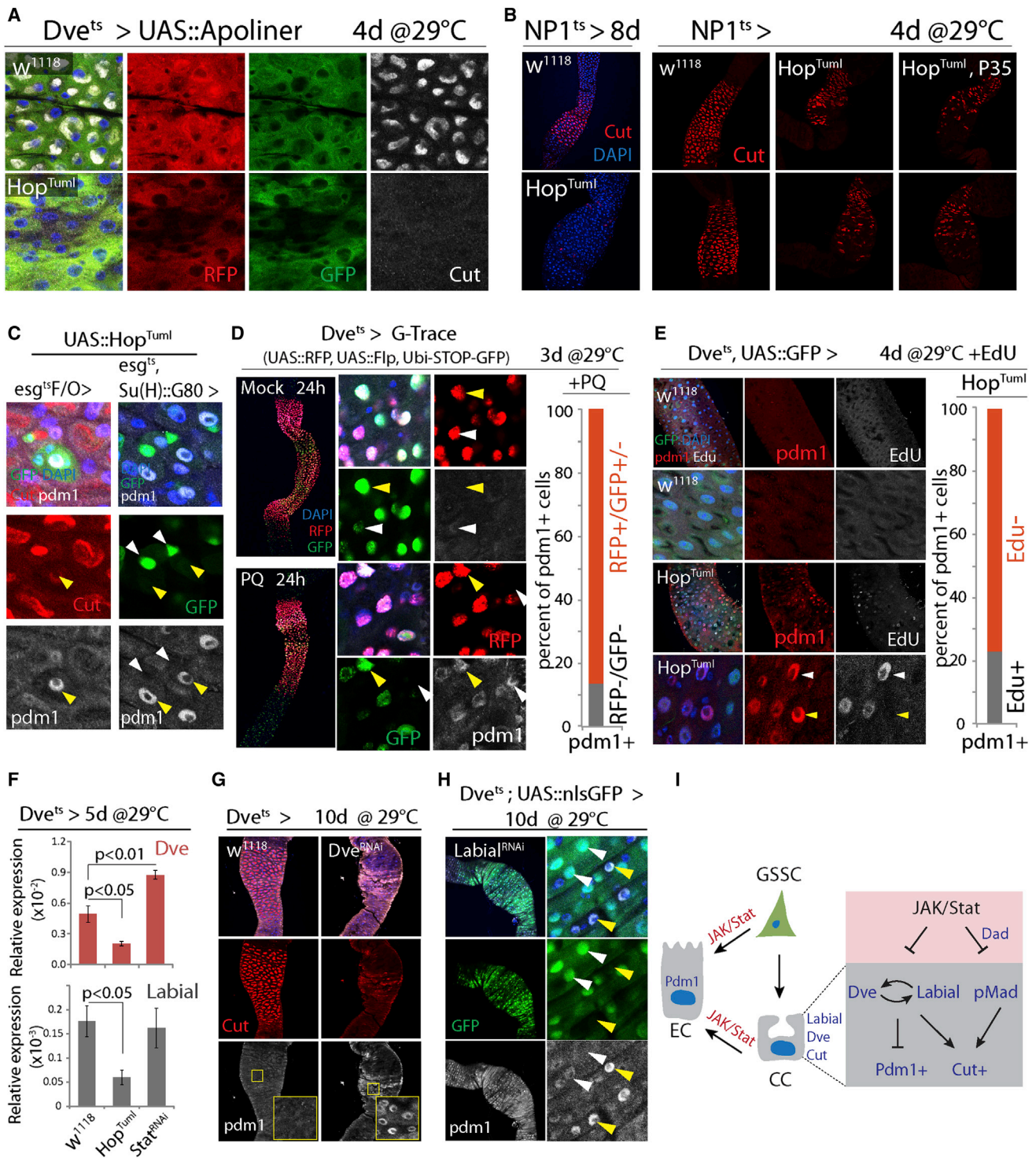


**Figure 4. Mechanisms of Metaplasia: GSSC Mis-differentiation and CC Trans-differentiation**

(A) Expression of Apoliner in the CCR. No apoptosis is observed in CCs expressing  $Hop^{TumI}$ . Representative images of seven flies per genotype.

(B) Loss of CCs (red) upon overexpression of  $Hop^{TumI}$  using  $NP1::Gal4^{ts}$ . Co-expression of P35 does not prevent CC loss. Representative images of nine flies per genotype.

(C)  $Pdm1^+$  cells (arrow) are generated in GSSC-derived clones (left;  $esg^{ts}F/O > Hop^{TumI}$ , green), or when  $Hop^{TumI}$  is overexpressed only in the GSSCs (right;  $esg::Gal4^{ts}$  with  $Su(H)::Gal80$ ). Note that GFP+ GSSCs (white arrow) do not express  $Pdm1$ .

(D) G-Trace expression was initiated by incubating flies at 29°C for 3 days before inducing  $Pdm1^+$  cells by Paraquat (PQ) treatment. All  $Dve^+$  cells express RFP (red), while GFP expression (green) remains mosaic, indicating that Flp-mediated recombination occurs only in a subset of these cells (yellow arrowhead strong

(legend continued on next page)

reduced dysplasia (Figures 5C–5E), and prevented the age-related decline in both food intake (CAFÉ assay [Ja et al., 2007]) and excretion (Figures 5F, 5G, S6D, and S6E). Flies in which Dome was knocked down using Dve::Gal4 further lived significantly longer than controls (Figure 6A). We confirmed the lifespan extension by limiting JAK/Stat signaling in the CCR using a newly generated RU486-responsive Geneswitch (McGuire et al., 2004b) driver based on *labial* regulatory regions (Labial::GS; Figure S7A) (Jenett et al., 2012). In response to RU486, this driver selectively induces UAS-linked transgene expression in the MM and is not expressed in other regions of the gut or in other tissues (Figures 6B and S7B). This driver thus allows selective repression of JAK/STAT components in the MM in a temporally controlled manner and allows for comparison of genetically identical sibling populations exposed to RU486 or vehicle. When Stat, Hop, or Dome were knocked down throughout adulthood using this driver, the percentage of old animals exhibiting a breakdown of intestinal barrier function (“Smurf” assay [Rera et al., 2012]) was reduced, and lifespan was consistently and significantly increased after RU486 supplementation (Figures 6C–6E and S7C). Reducing JAK/Stat activity in the CCR also extended lifespan of flies cultured on antibiotic food (Figure S7D), suggesting that maintenance of GI compartmentalization impacts lifespan not only by improving microbiota homeostasis but has additional beneficial effects. Flies cultured on antibiotic food generally have a longer lifespan than flies cultured on conventional food (Figures S7C and S7D), consistent with other studies (Brummel et al., 2004; Clark et al., 2015).

## DISCUSSION

Our results identify a critical role for the gastric region in managing commensal compartmentalization, composition, and load in the GI tract of adult flies. The importance of this function is reflected by the significant deleterious consequences of age-related epithelial metaplasia. Metaplasia of the gastric epithelium, caused by chronic inflammation (in the form of JAK/Stat activation), thus emerges as the origin of age-related pathophysiological changes in the gastrointestinal tract of *Drosophila*, highlighting the role of low-level inflammation as a driver of age-related pathologies (Figure 7). This observation, as well as insight from previous studies, provides a model for the molecular events driving the progression of age-related pathological changes in the intestinal epithelium (Figure 7) (Biteau et al., 2010; Clark et al., 2015; Guo et al., 2014; Rera et al., 2012).

Previous studies have linked age-related immunosenescence to microbiota dysbiosis and epithelial dysplasia and have identified the loss of barrier function as a significant step triggering changes in both load and composition of the intestinal microbiota, thus

increasing mortality (Clark et al., 2015; Guo et al., 2014). Our results introduce gastric metaplasia as an initiating age-related dysfunction that subsequently triggers the phenotypes discussed above. We propose that JAK/Stat-induced gastric metaplasia causes pH changes, resulting in dysbiosis and innate immune deregulation, and triggering a secondary inflammatory response that damages the epithelium and causes excessive ISC activity, leading to dysplasia and shortening lifespan (Guo et al., 2014). The lifespan extension observed when JAK/STAT was reduced in the CCR of sterile flies indicates broader beneficial consequences of this perturbation that may result from improved food digestion and nutrient assimilation. Furthermore, since microbes also have a beneficial effect on fly nutrition (Yamada et al., 2015), it is likely that the metabolic consequences of age-related gastric decline are complex and provide interesting grounds for future studies.

In humans, Barrett’s metaplasia, in which the esophageal squamous epithelium acquires properties that are reminiscent of the gastric or intestinal epithelium, is believed to be a cause of esophageal adenocarcinomas (Dvorak et al., 2011; Peters and Avisar, 2010), and metaplasia of the gastric mucosa has been associated with the progression from inflammation to dysplasia and carcinogenesis (Correa and Houghton, 2007). Barrett’s metaplasia and malignant transformation of intestinal progenitor cells has been linked to inflammation and JAK/Stat activation (Liu et al., 2013; Nguyen et al., 2010; Ullman and Itzkowitz, 2011), and in vertebrate airway epithelia, JAK/Stat activating inflammatory cytokines have been implicated in asthma-induced metaplasias (Ren et al., 2013). Pre-malignant intestinal-type metaplasias in the gastric region are common in the general population and their incidence increases with age (Zullo et al., 2012), and our results suggest that such metaplasias occur as a consequence of basal inflammation in the aging organism. Accordingly, age-related loss of tissue homeostasis and cancer progression is associated with an inflammatory state (Grivennikov et al., 2010; Mantovani, 2009; Shaw et al., 2013). Based on this model, it can be anticipated that interventions targeting basal inflammation, and thus preventing chronic activation of JAK/Stat signaling, may significantly promote tissue maintenance, regenerative capacity, and tissue homeostasis, ultimately extending lifespan.

## EXPERIMENTAL PROCEDURES

### Fly Lines and Husbandry

See Supplemental Experimental Procedures.

### Immunostaining, TUNEL Staining, and Microscopy

Female guts were dissected in 1 × PBS, fixed for 45 min at 25°C in fixative, washed for 1 hr at 4°C in washing buffer, and then incubated at 4°C in primary antibodies overnight and secondary antibodies for 4 hr. TUNEL staining was performed using In Situ Cell Death Detection Kit (Roche, 12156792910).

GFP, recombined; white arrowhead background GFP, non-recombined). Graph shows the ratio of Pdm1+ cells that express RFP and/or GFP. n = 239 cells from 3 guts.

(E) EdU incorporation analysis to determine whether formation of Pdm1+ cells in the CCR involves DNA synthesis. Among induced Pdm1+ cells (red), 23% are EdU positive (white arrowhead), while 77% are EdU negative (yellow arrowhead). n = 126 cells from 4 guts. In *w<sup>1118</sup>* CCRs, no Pdm1 or EdU is detected.

(F) qRT-PCR showing *Dve* and *Labial* expression in CCRs of indicated genotypes. Averages and SEM (t test). n = 3 biological replicates.

(G) *Dve* knockdown results in loss of CCs (red) and generation of Pdm1+ cells (white).

(H) *Labial* knockdown results in loss of CCs (red) and generation of Pdm1+ cells (white). Note that in the high Pdm1+ cells, GFP (*Dve::Gal4* >) signal is reduced (yellow arrow) compared to low- or non-Pdm1 cells (white arrow).

(I) Model for the role of JAK/Stat signaling in promoting mis- and trans-differentiation of CCR cells.

See also Figures S4 and S5.

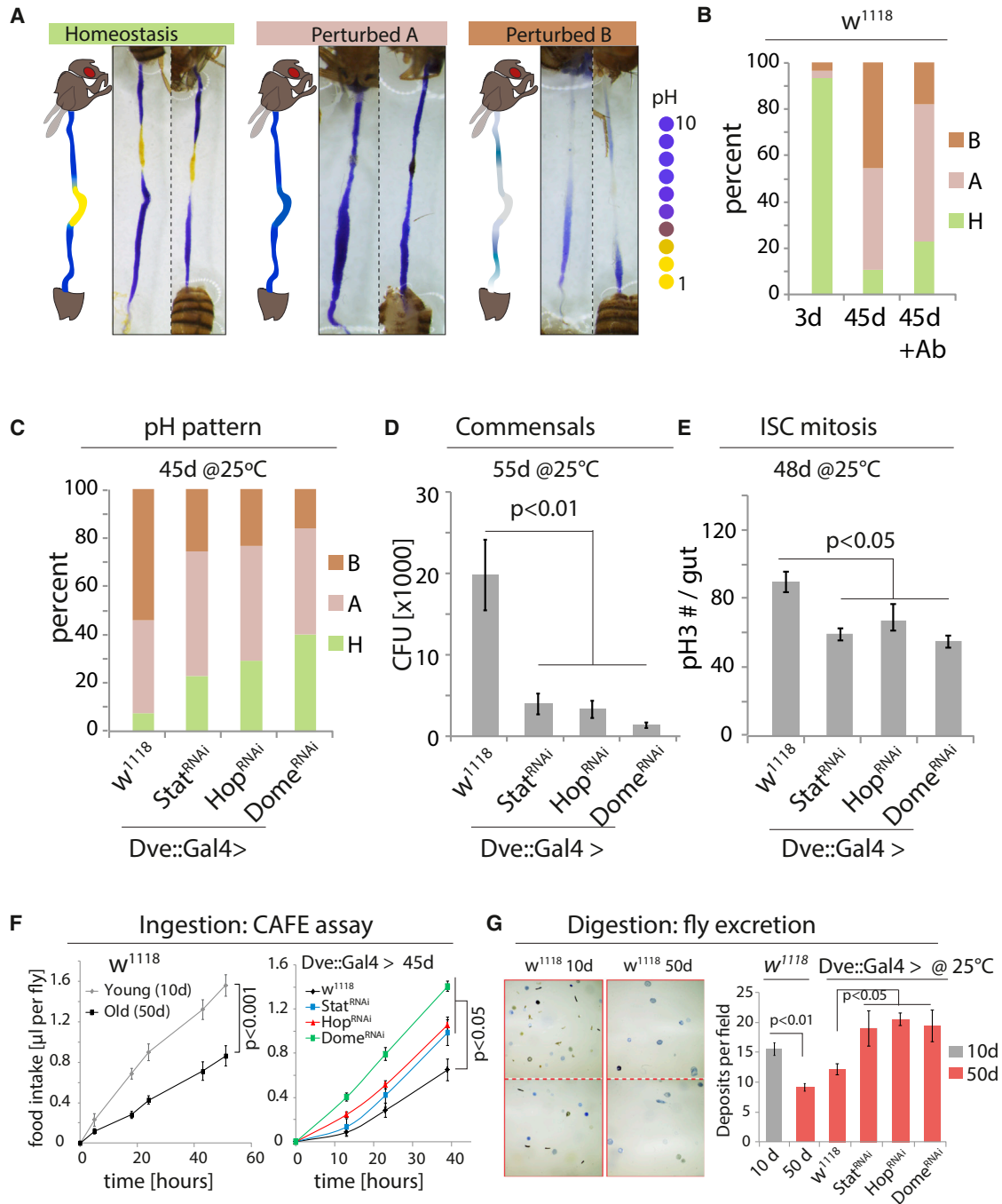


**Figure 5. Inhibiting JAK/Stat Signaling in the CCR Promotes Gut Function and Homeostasis**

(A) GI tracts of flies fed the pH indicator Bromophenol Blue. Three phenotypic categories can be distinguished: homeostasis, a well-defined acidic CCR is flanked by basic AM and PM; "Perturbed A," the acidic region is lost and the whole gut is basic; "Perturbed B," the strongly acidic region is lost, while the rest of the gut also becomes less basic (weak blue).

(B) Quantification of the three phenotypes in flies of indicated conditions. +Ab, Antibiotic treatment.  $n = 28, 57, 39$ . Representative of three independent experiments.

(C–E) Rescue of pH homeostasis (C;  $n = 13, 25, 17, 39$ ), commensal dysbiosis (D;  $n = 10$  each), and epithelial dysplasia (E; pH3+ cells in the gut,  $n = 12, 20, 12, 12$ ) in old flies expressing  $Stat^{RNAi}$ ,  $Hop^{RNAi}$ , or  $Dome^{RNAi}$  in the CCR. CFU, colony-forming unit. Representative of three independent experiments.

(F) Food intake measured using CAFE assay. Averages and SEM (t test).  $n = 18$  flies from 6 replicates ( $w^{1118}$ ) or 21 flies from 7 replicates (other genotypes).

(G) Excretion from flies fed Bromophenol blue. Images of deposits and quantification of deposit numbers are shown. Excretions are quantified in 8 to 24 fields for each group of 12 flies. Averages and SEM (t test).  $n = 24, 24, 8, 12, 12, 12$  fields.

See also Figure S6.

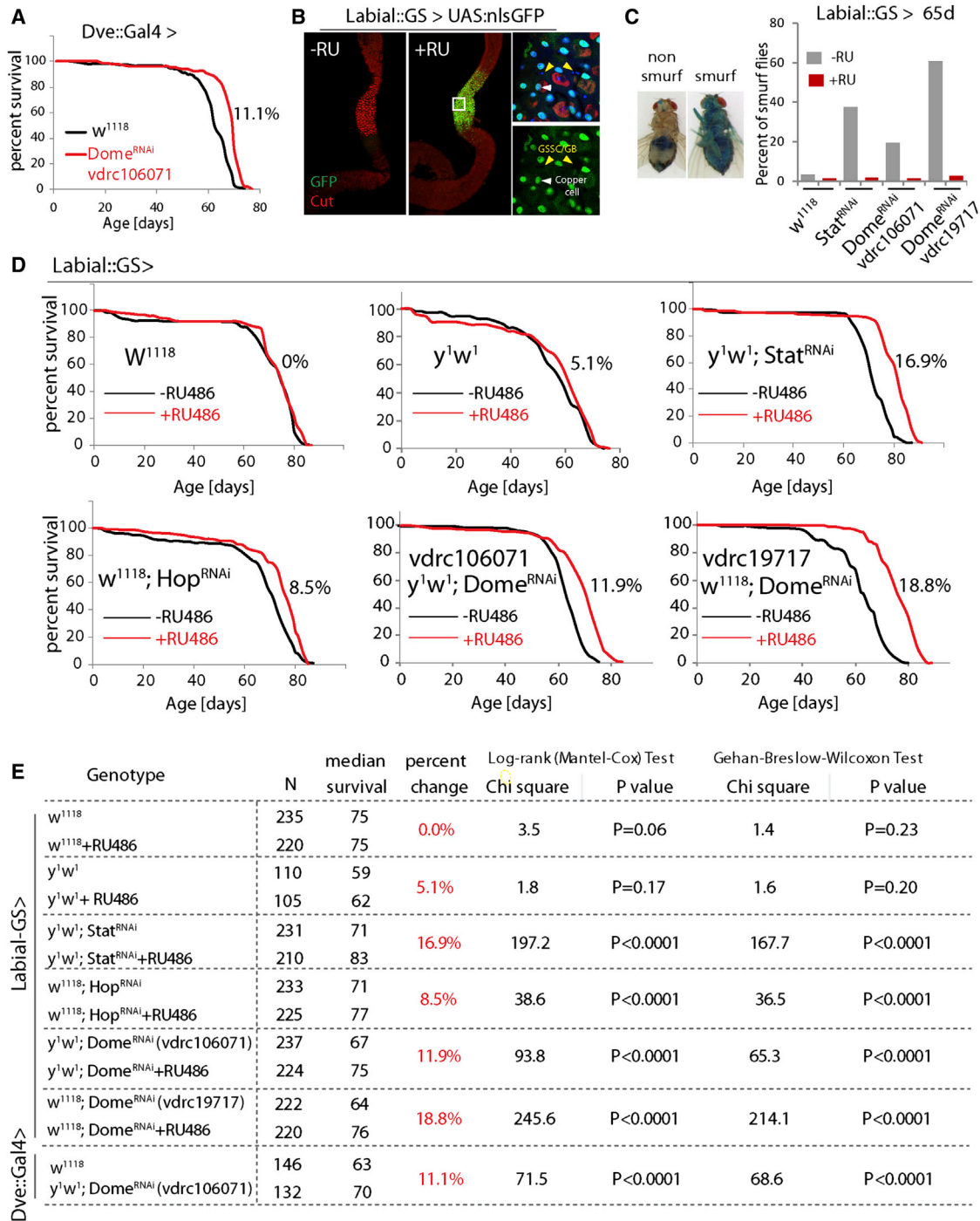


**Figure 6. Inhibiting JAK/Stat Signaling in the CCR Extends Lifespan**

(A) Demography of flies expressing Dome<sup>RNAi</sup> in the CCR (*w<sup>1118</sup>* as control). The percent change of median lifespan is indicated. All flies are female.

(B) Characterization of Labial-GeneSwitch. In response to RU486, UAS::GFP expression is observed in the CCR specifically. High magnification (right) shows that this expression is in differentiated polyploid cells (including CCs, white arrowhead) but not in diploid cells (GSSCs and GBs, yellow arrowhead). Representative images of seven flies for each condition.

(C) Smurf assay for gut permeability of 65-day-old flies. Percent of Smurf flies are shown. n = 137, 139, 122, 121, 123, 147, 128, 143.

(D) Demography of flies expressing Stat<sup>RNAi</sup>, Hop<sup>RNAi</sup>, or two different Dome<sup>RNAi</sup> constructs under the control of Labial::GS, with *w<sup>1118</sup>* and *y<sup>1</sup>w<sup>1</sup>* as control. Graphs are combined from independent populations (only one population for *y<sup>1</sup>w<sup>1</sup>*) of F1 progeny from Labial::GS crossed to the indicated transgenes or to *w<sup>1118</sup>* and *y<sup>1</sup>w<sup>1</sup>* (control). The percent changes of median lifespan are indicated. All flies are female. Survival data were analyzed using GraphPad Prism.

(E) Summary of parameters and statistics of the demography shown in (A) and (D). Survival data was analyzed using GraphPad Prism.

See also Figure S7.

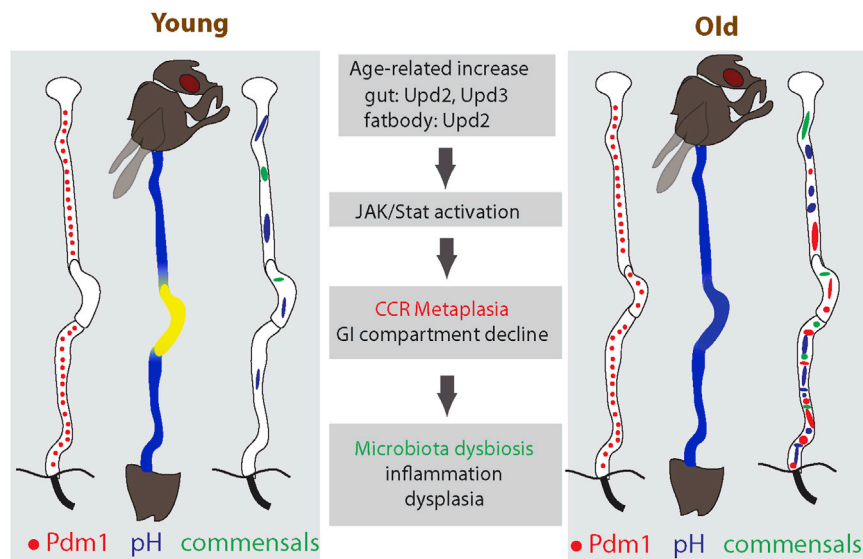


**Figure 7. Origin and Pathophysiological Consequences of Age-Related Gastric Metaplasia**

Age-related increase of JAK/Stat activity, induced by increased cytokines from the gut and/or fat body, causes metaplasia in the CCR. This results in pH imbalance, promoting commensal dysbiosis, inflammation, and dysplasia in the old intestine.

3,388 bp promoter region corresponding to that line was amplified (primers: 5'-CCACCCCTG GAATCGGTAATTTCT-3' and 5'-GAGCGCGTGTG ACAAGATGGATAAA-3') and inserted into p[UAS-GeneSwitch] using MluI and NotI sites (Osterwalder et al., 2001). Transgenic animals were generated in the  $w^{1118}$  background using standard P element transgenesis (GENETIC SERVICES).

#### 16S rDNA Sequencing and PCA Analysis

See [Supplemental Experimental Procedures](#) for the preparation of sequencing library.

Illumina Miseq paired-end ( $2 \times 300$  bp) sequencing was performed and Miseq Reporter Software was used for primary analysis and classification based on Greengenes database (<http://greengenes.lbl.gov/>). We noticed that for samples with low numbers of bacteria, e.g., young wild-type guts, there were high percentages of unclassified species. Further analysis (by Tal Ronnen Oron) of DNA sequences responsible for these unclassified species revealed that these DNA sequences were from the *Drosophila* genome, presumably due to non-specific amplification during the preparation of 16S sequencing libraries; these sequences were excluded in subsequent analysis. The percentage of each classified bacterium at the species level was used for principle component analysis (PCA) using MAT-LAB (princomp command), and Prism software was used for plotting the data.

#### Commensal DNA Concentration

See [Supplemental Experimental Procedures](#).

#### RFP-Tagged Lactobacillus

The plasmid pLEM415-ldhL-mRFP1 (Bao et al., 2013) was used for transformation of one strain of commensal *Lactobacillus*, which was isolated and cultured from wild-type flies. The procedure of competent cell preparation and electrical transformation has been described (Bao et al., 2013). The transformed strain was later identified as *Lactobacillus plantarum* by sequencing the 16S rRNA gene.

#### RT-PCR and Primer Sequences

See [Supplemental Experimental Procedures](#).

#### Cafe Assay and Fly Excretion Measurement

The Cafe and fly excretion assays were performed as described in Deshpande et al. (2014) and Cognigni et al. (2011), respectively. See [Supplemental Experimental Procedures](#) for details.

#### Statistical Methods

Statistical analysis was performed using GraphPad Prism5 and Microsoft Excel. Statistical methods used and sample sizes are listed in figure legends. Sample sizes were chosen empirically based on observed effect sizes.

#### SUPPLEMENTAL INFORMATION

Supplemental Information includes Supplemental Experimental Procedures and seven figures and can be found with this article online at <http://dx.doi.org/10.1016/j.chom.2016.01.008>.

Images were taken on a Zeiss LSM 700 confocal microscope and processed using Adobe Photoshop, Illustrator, and Image J.

See [Supplemental Experimental Procedures](#) for details about fixative, washing buffer, and antibodies.

#### pH Indicator, Blue Dye, Paraquat Treatment, and Lactobacillus Feeding

100  $\mu$ l of 2% Bromophenol blue sodium (pH indicator, Sigma), or 5% sucrose  $\pm$  80 mM paraquat (methyl viologen, Sigma) was added to a food vial and pipet tip was used to poke 4–6 holes in the food to allow full absorption. Flies were fed overnight. For *Lactobacillus* feeding, flies were fed 400  $\mu$ l of concentrated bacteria (OD100, in 5% sucrose) mixed with either 100  $\mu$ l 2% pH indicator or 2.5% blue dye (FD&C Blue 1, SENSIENT) in filter paper for overnight. During dissection, the fly head and posterior cuticle was left intact to prevent dye leakage. Images were taken immediately after each gut was dissected. Long-term exposure of flies with pH indicator on CO<sub>2</sub> pad will disturb normal pH patterns.

#### Edu Incorporation

The Click-iT Edu Imaging Kit from Invitrogen was applied. Briefly, 100  $\mu$ l Edu solution (100  $\mu$ M, diluted with water from 10 mM stock) was added to a food vial (pipet tip was used to poke 4–6 holes in the food to allow full absorption of the solution). Flies were fed Edu food at 29°C for 4 days.

#### Demography and Axenic Fly Culture

The procedure was performed as described (Guo et al., 2014). See [Supplemental Experimental Procedures](#) for details.

#### *esg*<sup>tsF/O</sup> and MARCM Clone Induction

Because of the intrinsic quiescence of gastric stem cells, the frequency of clone formation in the CCR is low. Double heat-shock (45 min at 37°C, 3 hr at 25°C, then 45 min at 37°C) was applied to induce enough clones for analysis.

See [Supplemental Experimental Procedures](#) for details.

#### Commensal Quantification and Selective Plates

The procedure was performed as described (Guo et al., 2014). In brief, dissected guts were homogenized in 200 ml sterile 1  $\times$  PBS and plated onto selective plates, which were incubated at 29°C for 48–72 hr before the colony-forming units were quantified. See [Supplemental Experimental Procedures](#) for recipes of selective plates.

#### Generation of Labial-GeneSwitch

A collection of Janelia-Gal4 lines with varied labial promoter regions were screened (Jenett et al., 2012) for their expression in the intestine, and one line (BL49323) was found to be expressed most specifically in the CCR. The

## AUTHOR CONTRIBUTIONS

H.L. and H.J. designed and conceived the study, H.L. and Y.Q. performed all experiments, and H.J. and H.L. analyzed data and wrote the manuscript.

## ACKNOWLEDGMENTS

This work was funded by the National Institute on Aging (R01 AG028127), the National Institute on General Medical Sciences (R01 GM100196), and the American Federation for Aging Research (Breakthroughs in Gerontology award to H.J.). We would like to thank the Vienna *Drosophila* RNAi Center and the Bloomington Stock Center for flies, and Developmental Studies Hybridoma Bank for antibodies. We thank Rachel Brem and Tal Ronnen Oron for bioinformatics support, Jason Karpac for valuable comments on the manuscript, and H.J. lab members for discussion.

Received: October 15, 2015

Revised: December 26, 2015

Accepted: January 22, 2016

Published: February 10, 2016

## REFERENCES

- Alic, N., Giannakou, M.E., Papatheodorou, I., Hodginott, M.P., Andrews, T.D., Bolukbasi, E., and Partridge, L. (2014). Interplay of dFOXO and two ETS-family transcription factors determines lifespan in *Drosophila melanogaster*. *PLoS Genet.* *10*, e1004619.
- Ayyaz, A., and Jasper, H. (2013). Intestinal inflammation and stem cell homeostasis in aging *Drosophila melanogaster*. *Front. Cell. Infect. Microbiol.* *3*, 98.
- Bach, E.A., Ekas, L.A., Ayala-Camargo, A., Flaherty, M.S., Lee, H., Perrimon, N., and Baeg, G.H. (2007). GFP reporters detect the activation of the *Drosophila* JAK/STAT pathway in vivo. *Gene Expr. Patterns* *7*, 323–331.
- Bao, S., Zhu, L., Zhuang, Q., Wang, L., Xu, P.X., Itoh, K., Holzman, I.R., and Lin, J. (2013). Distribution dynamics of recombinant *Lactobacillus* in the gastrointestinal tract of neonatal rats. *PLoS ONE* *8*, e60007.
- Bardet, P.L., Kolahgar, G., Mynett, A., Miguel-Aliaga, I., Briscoe, J., Meier, P., and Vincent, J.P. (2008). A fluorescent reporter of caspase activity for live imaging. *Proc. Natl. Acad. Sci. USA* *105*, 13901–13905.
- Barker, N., Bartfeld, S., and Clevers, H. (2010). Tissue-resident adult stem cell populations of rapidly self-renewing organs. *Cell Stem Cell* *7*, 656–670.
- Biteau, B., Hochmuth, C.E., and Jasper, H. (2008). JNK activity in somatic stem cells causes loss of tissue homeostasis in the aging *Drosophila* gut. *Cell Stem Cell* *3*, 442–455.
- Biteau, B., Karpac, J., Supoyo, S., Degennaro, M., Lehmann, R., and Jasper, H. (2010). Lifespan extension by preserving proliferative homeostasis in *Drosophila*. *PLoS Genet.* *6*, e1001159.
- Biteau, B., Hochmuth, C.E., and Jasper, H. (2011a). Maintaining tissue homeostasis: dynamic control of somatic stem cell activity. *Cell Stem Cell* *9*, 402–411.
- Biteau, B., Karpac, J., Hwangbo, D., and Jasper, H. (2011b). Regulation of *Drosophila* lifespan by JNK signaling. *Exp. Gerontol.* *46*, 349–354.
- Blum, J.E., Fischer, C.N., Miles, J., and Handelsman, J. (2013). Frequent replenishment sustains the beneficial microbiome of *Drosophila melanogaster*. *MBio* *4*, e00860–e13.
- Broderick, N.A., Buchon, N., and Lemaître, B. (2014). Microbiota-induced changes in *drosophila melanogaster* host gene expression and gut morphology. *MBio* *5*, e01117–e14.
- Brummel, T., Ching, A., Seroude, L., Simon, A.F., and Benzer, S. (2004). *Drosophila* lifespan enhancement by exogenous bacteria. *Proc. Natl. Acad. Sci. USA* *101*, 12974–12979.
- Buchon, N., Broderick, N.A., Chakrabarti, S., and Lemaître, B. (2009). Invasive and indigenous microbiota impact intestinal stem cell activity through multiple pathways in *Drosophila*. *Genes Dev.* *23*, 2333–2344.
- Buchon, N., Osman, D., David, F.P., Fang, H.Y., Boquete, J.P., Deplancke, B., and Lemaître, B. (2013). Morphological and molecular characterization of adult midgut compartmentalization in *Drosophila*. *Cell Rep.* *3*, 1725–1738.
- Claesson, M.J., Cusack, S., O'Sullivan, O., Greene-Diniz, R., de Weerd, H., Flannery, E., Marchesi, J.R., Falush, D., Dinan, T., Fitzgerald, G., et al. (2011). Composition, variability, and temporal stability of the intestinal microbiota of the elderly. *Proc. Natl. Acad. Sci. USA* *108* (Suppl 1), 4586–4591.
- Claesson, M.J., Jeffery, I.B., Conde, S., Power, S.E., O'Connor, E.M., Cusack, S., Harris, H.M., Coakley, M., Lakshminarayanan, B., O'Sullivan, O., et al. (2012). Gut microbiota composition correlates with diet and health in the elderly. *Nature* *488*, 178–184.
- Clark, R.I., Salazar, A., Yamada, R., Fitz-Gibbon, S., Morselli, M., Alcaraz, J., Rana, A., Rera, M., Pellegrini, M., Ja, W.W., and Walker, D.W. (2015). Distinct Shifts in Microbiota Composition during *Drosophila* Aging Impair Intestinal Function and Drive Mortality. *Cell Rep.* *12*, 1656–1667.
- Classen, A.K., Bunker, B.D., Harvey, K.F., Vaccari, T., and Bilder, D. (2009). A tumor suppressor activity of *Drosophila* Polycomb genes mediated by JAK-STAT signaling. *Nat. Genet.* *41*, 1150–1155.
- Clemente, J.C., Ursell, L.K., Parfrey, L.W., and Knight, R. (2012). The impact of the gut microbiota on human health: an integrative view. *Cell* *148*, 1258–1270.
- Cognigni, P., Bailey, A.P., and Miguel-Aliaga, I. (2011). Enteric neurons and systemic signals couple nutritional and reproductive status with intestinal homeostasis. *Cell Metab.* *13*, 92–104.
- Correa, P., and Houghton, J. (2007). Carcinogenesis of *Helicobacter pylori*. *Gastroenterology* *133*, 659–672.
- David, L.A., Maurice, C.F., Carmody, R.N., Gootenberg, D.B., Button, J.E., Wolfe, B.E., Ling, A.V., Devlin, A.S., Varma, Y., Fischbach, M.A., et al. (2014). Diet rapidly and reproducibly alters the human gut microbiome. *Nature* *505*, 559–563.
- Deshpande, S.A., Carvalho, G.B., Amador, A., Phillips, A.M., Hoxha, S., Lizotte, K.J., and Ja, W.W. (2014). Quantifying *Drosophila* food intake: comparative analysis of current methodology. *Nat. Methods* *11*, 535–540.
- Dubreuil, R.R. (2004). Copper cells and stomach acid secretion in the *Drosophila* midgut. *Int. J. Biochem. Cell Biol.* *36*, 745–752.
- Dvorak, K., Goldman, A., Kong, J., Lynch, J.P., Hutchinson, L., Houghton, J.M., Chen, H., Chen, X., Krishnadath, K.K., and Westra, W.M. (2011). Molecular mechanisms of Barrett's esophagus and adenocarcinoma. *Ann. N Y Acad. Sci.* *1232*, 381–391.
- Evans, C.J., Olson, J.M., Ngo, K.T., Kim, E., Lee, N.E., Kuoy, E., Patananan, A.N., Sitz, D., Tran, P., Do, M.T., et al. (2009). G-TRACE: rapid Gal4-based cell lineage analysis in *Drosophila*. *Nat. Methods* *6*, 603–605.
- Grivnennikov, S.I., Greten, F.R., and Karin, M. (2010). Immunity, inflammation, and cancer. *Cell* *140*, 883–899.
- Guo, Z., Driver, I., and Ohlstein, B. (2013). Injury-induced BMP signaling negatively regulates *Drosophila* midgut homeostasis. *J. Cell Biol.* *207*, 945–961.
- Guo, L., Karpac, J., Tran, S.L., and Jasper, H. (2014). PGRP-SC2 promotes gut immune homeostasis to limit commensal dysbiosis and extend lifespan. *Cell* *156*, 109–122.
- Hanratty, W.P., and Dearolf, C.R. (1993). The *Drosophila* Tumorous-lethal hematopoietic oncogene is a dominant mutation in the hopscotch locus. *Mol. Gen. Genet.* *238*, 33–37.
- Hwangbo, D.S., Gershman, B., Tu, M.P., Palmer, M., and Tatar, M. (2004). *Drosophila* dFOXO controls lifespan and regulates insulin signalling in brain and fat body. *Nature* *429*, 562–566.
- Ja, W.W., Carvalho, G.B., Mak, E.M., de la Rosa, N.N., Fang, A.Y., Liong, J.C., Brummel, T., and Benzer, S. (2007). Prandiology of *Drosophila* and the CAFE assay. *Proc. Natl. Acad. Sci. USA* *104*, 8253–8256.
- Jenett, A., Rubin, G.M., Ngo, T.T., Shepherd, D., Murphy, C., Dionne, H., Pfeiffer, B.D., Cavallaro, A., Hall, D., Jeter, J., et al. (2012). A GAL4-driver line resource for *Drosophila* neurobiology. *Cell Rep.* *2*, 991–1001.
- Jiang, H., Patel, P.H., Kohlmaier, A., Grenley, M.O., McEwen, D.G., and Edgar, B.A. (2009). Cytokine/Jak/Stat signaling mediates regeneration and homeostasis in the *Drosophila* midgut. *Cell* *137*, 1343–1355.
- Korzelius, J., Naumann, S.K., Loza-Coll, M.A., Chan, J.S., Dutta, D., Oberheim, J., Gläßer, C., Southall, T.D., Brand, A.H., Jones, D.L., and Edgar, B.A. (2014). Escargot maintains stemness and suppresses differentiation in *Drosophila* intestinal stem cells. *EMBO J.* *33*, 2967–2982.

- Lee, W.C., Beebe, K., Sudmeier, L., and Micchelli, C.A. (2009). Adenomatous polyposis coli regulates *Drosophila* intestinal stem cell proliferation. *Development* **136**, 2255–2264.
- Lemaitre, B., and Miguel-Aliaga, I. (2013). The digestive tract of *Drosophila melanogaster*. *Annu. Rev. Genet.* **47**, 377–404.
- Li, H., Qi, Y., and Jasper, H. (2013). Dpp signaling determines regional stem cell identity in the regenerating adult *Drosophila* gastrointestinal tract. *Cell Rep.* **4**, 10–18.
- Lin, W.S., Huang, C.W., Song, Y.S., Yen, J.H., Kuo, P.C., Yeh, S.R., Lin, H.Y., Fu, T.F., Wu, M.S., Wang, H.D., and Wang, P.Y. (2015). Reduced Gut Acidity Induces an Obese-Like Phenotype in *Drosophila melanogaster* and in Mice. *PLoS ONE* **10**, e0139722.
- Liu, K., Jiang, M., Lu, Y., Chen, H., Sun, J., Wu, S., Ku, W.Y., Nakagawa, H., Kita, Y., Natsugoe, S., et al. (2013). Sox2 cooperates with inflammation-mediated Stat3 activation in the malignant transformation of foregut basal progenitor cells. *Cell Stem Cell* **12**, 304–315.
- Mantovani, A. (2009). Cancer: Inflaming metastasis. *Nature* **457**, 36–37.
- Marianes, A., and Spradling, A.C. (2013). Physiological and stem cell compartmentalization within the *Drosophila* midgut. *eLife* **2**, e00886.
- McGuire, S.E., Mao, Z., and Davis, R.L. (2004a). Spatiotemporal gene expression targeting with the TARGET and gene-switch systems in *Drosophila*. *Sci. STKE* **2004**, pl6.
- McGuire, S.E., Roman, G., and Davis, R.L. (2004b). Gene expression systems in *Drosophila*: a synthesis of time and space. *Trends Genet.* **20**, 384–391.
- Nguyen, G.H., Schetter, A.J., Chou, D.B., Bowman, E.D., Zhao, R., Hawkes, J.E., Mathé, E.A., Kumamoto, K., Zhao, Y., Budhu, A., et al. (2010). Inflammatory and microRNA gene expression as prognostic classifier of Barrett's-associated esophageal adenocarcinoma. *Clin. Cancer Res.* **16**, 5824–5834.
- Osman, D., Buchon, N., Chakrabarti, S., Huang, Y.T., Su, W.C., Poidevin, M., Tsai, Y.C., and Lemaitre, B. (2012). Autocrine and paracrine unpaired signaling regulate intestinal stem cell maintenance and division. *J. Cell Sci.* **125**, 5944–5949.
- Osterwalder, T., Yoon, K.S., White, B.H., and Keshishian, H. (2001). A conditional tissue-specific transgene expression system using inducible GAL4. *Proc. Natl. Acad. Sci. USA* **98**, 12596–12601.
- Peters, J.H., and Avisar, N. (2010). The molecular pathogenesis of Barrett's esophagus: common signaling pathways in embryogenesis metaplasia and neoplasia. *J. Gastrointest. Surg.* **14** (Suppl 1), S81–S87.
- Rajan, A., and Perrimon, N. (2012). *Drosophila* cytokine unpaired 2 regulates physiological homeostasis by remotely controlling insulin secretion. *Cell* **151**, 123–137.
- Ren, X., Shah, T.A., Ustiyani, V., Zhang, Y., Shinn, J., Chen, G., Whitsett, J.A., Kalin, T.V., and Kalinichenko, V.V. (2013). FOXM1 promotes allergen-induced goblet cell metaplasia and pulmonary inflammation. *Mol. Cell. Biol.* **33**, 371–386.
- Rera, M., Clark, R.I., and Walker, D.W. (2012). Intestinal barrier dysfunction links metabolic and inflammatory markers of aging to death in *Drosophila*. *Proc. Natl. Acad. Sci. USA* **109**, 21528–21533.
- Ryu, J.H., Kim, S.H., Lee, H.Y., Bai, J.Y., Nam, Y.D., Bae, J.W., Lee, D.G., Shin, S.C., Ha, E.M., and Lee, W.J. (2008). Innate immune homeostasis by the homeobox gene caudal and commensal-gut mutualism in *Drosophila*. *Science* **319**, 777–782.
- Shaw, A.C., Goldstein, D.R., and Montgomery, R.R. (2013). Age-dependent dysregulation of innate immunity. *Nat. Rev. Immunol.* **13**, 875–887.
- Strand, M., and Micchelli, C.A. (2011). Quiescent gastric stem cells maintain the adult *Drosophila* stomach. *Proc. Natl. Acad. Sci. USA* **108**, 17696–17701.
- Ullman, T.A., and Itzkowitz, S.H. (2011). Intestinal inflammation and cancer. *Gastroenterology* **140**, 1807–1816.
- Wang, L., Zeng, X., Ryoo, H.D., and Jasper, H. (2014). Integration of UPRER and oxidative stress signaling in the control of intestinal stem cell proliferation. *PLoS Genet.* **10**, e1004568.
- Yamada, R., Deshpande, S.A., Bruce, K.D., Mak, E.M., and Ja, W.W. (2015). Microbes Promote Amino Acid Harvest to Rescue Undernutrition in *Drosophila*. *Cell Rep.* Published online February 12, 2015. <http://dx.doi.org/10.1016/j.celrep.2015.01.018>.
- Zhou, F., Rasmussen, A., Lee, S., and Agaisse, H. (2013). The UPD3 cytokine couples environmental challenge and intestinal stem cell division through modulation of JAK/STAT signaling in the stem cell microenvironment. *Dev. Biol.* **373**, 383–393.
- Zullo, A., Hassan, C., Romiti, A., Giusto, M., Guerriero, C., Lorenzetti, R., Campo, S.M., and Tomao, S. (2012). Follow-up of intestinal metaplasia in the stomach: When, how and why. *World J. Gastrointest. Oncol.* **4**, 30–36.